Bowling Green State University
ScholarWorks@BGSU

Chemistry Faculty Publications | Chemistry

10-2011

Photoinduced Electron Transfer In Naphthalimide-pyridine Systems: Effect Of Proton Transfer On Charge Recombination Efficiencies

Pavel Kucheryavy

Renat Khatmullin

Ekaterina Mirzakulova

Dapeng Zhou

Ksenija D. Glusac
Bowling Green State University, kglusac@bgsu.edu

Follow this and additional works at: https://scholarworks.bgsu.edu/chem_pub

Part of the Chemistry Commons

Repository Citation

Kucheryavy, Pavel; Khatmullin, Renat; Mirzakulova, Ekaterina; Zhou, Dapeng; and Glusac, Ksenija D., "Photoinduced Electron Transfer In Naphthalimide-pyridine Systems: Effect Of Proton Transfer On Charge Recombination Efficiencies" (2011). *Chemistry Faculty Publications*. 113.
https://scholarworks.bgsu.edu/chem_pub/113

This Article is brought to you for free and open access by the Chemistry at ScholarWorks@BGSU. It has been accepted for inclusion in Chemistry Faculty Publications by an authorized administrator of ScholarWorks@BGSU.

THE JOURNAL OF PHYSICAL CHEMISTRY A

ARTICLE

pubs.acs.org/JPCA

Photoinduced Electron Transfer in Naphthalimide-Pyridine Systems: Effect of Proton Transfer on Charge Recombination Efficiencies

Pavel Kucheryavy, Renat Khatmullin, Ekaterina Mirzakulova, Dapeng Zhou, and Ksenija D. Glusac*

Department of Chemistry, Bowling Green State University, Bowling Green, OH 43403

ABSTRACT: We studied the effect of proton-coupled electron transfer on lifetimes of the charge-separated radicals produced upon light irradiation of the thiomethyl-naphthalimide donor SMe-NI-H in the presence of nitro-cyano-pyridine acceptor (NO_2-CN-PYR). The dynamics of electron and proton transfer were studied using femtosecond pump−probe spectroscopy in the UV/vis range. We find that the photoinduced electron transfer between excited SMe-NI-H and NO_2-CN-PYR occurs with a rate of $1.1 \times 10^9\ s^{-1}$ to produce radical ions SMe-NI-H$^{\bullet+}$ and NO_2-CN-PYR$^{\bullet-}$. These initially produced radical ions in a solvent cage do not undergo a proton transfer, possibly due to unfavorable geometry between N−H proton of the naphthalimide and aromatic N-atom of the pyridine. Some of the radical ions in the solvent cage recombine with a rate of $2.3 \times 10^{10}\ s^{-1}$, while some escape the solvent cage and recombine at a lower rate ($k = 4.27 \times 10^8\ s^{-1}$). The radical ions that escape the solvent cage undergo proton transfer to produce neutral radicals SMe-NI$^{\bullet}$ and NO_2-CN-PYR-H$^{\bullet}$. Because neutral radicals are not attracted to each other by electrostatic interactions, their recombination is slower that the recombination of the radical ions formed in model compounds that can undergo only electron transfer (SMe-NI-Me and NO_2-CN-PYR, $k = 1.2 \times 10^9\ s^{-1}$). The results of our study demonstrate that proton-coupled electron transfer can be used as an efficient method to achieve long-lived charge separation in light-driven processes.

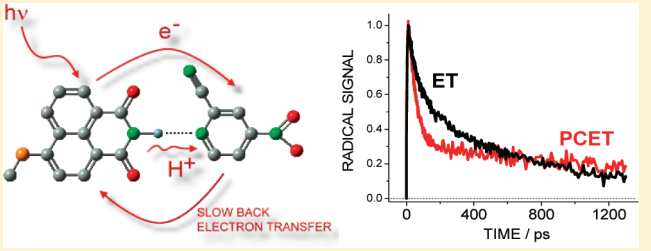

INTRODUCTION

Achieving long-lived charge separation (LLCS) is crucial for solar energy utilization. In natural photosynthetic organisms, LLCS is accomplished by a series of electron transfer steps to spatially separate radical ions.[1] Within less than a nanosecond, oxidized and reduced species are separated by almost 30 Å. Because electron transfer rates fall off exponentially with distance, spatial separation of radical ions reduces drastically the rate of charge recombination, which is demonstrated by a nearly 100% quantum efficiency of charge separation in photosynthetic reaction centers. Inspired by the efficiency of photosynthetic organisms, chemists have developed many artificial donor−acceptor dyads and triads that achieve LLCS by spatially separating the charges.[2−4] Most commonly used components for artificial photosynthetic triads include porphyrins as light absorbers, quinones or methyl-viologens as electron acceptors, and carotenoids or amines as electron donors. The lifetimes of charge separated states in these systems extends even to the millisecond time scale.

Another interesting approach to LLCS is to decrease the reorganization energy required for electron transfer. If reorganization energy λ is small, the charge recombination will occur deeply in the Marcus inverted region,[5] which drastically increases lifetimes of charge separated ions. The efficiency of this approach has been demonstrated by using fullerenes as electron acceptors.[6,7] Due to the high symmetry and rigid structure of fullerenes, the accepted electron is highly delocalized, leading to small solvent and nuclear reorganization energy required to accommodate the newly produced charge (for example, λ = 0.66 eV for Zn-porphyrin/C60 dyad[6]). In organic photovoltaics, the use of C60 as an electron acceptor has significantly increased the solar conversion efficiency of a device.[8,9]

A third approach to LLCS involves a chemical modification of radical ions formed upon electron transfer. For example, I^-/I_3^- couple was shown to be an excellent redox mediator in dye-sensitized solar cells (DSSC).[10] The iodide/triiodide couple is used for the reduction of the oxidized Ru dye (iodide is oxidized in this process: $2I^- \rightarrow I_2^{\bullet-} + e^-$). The $I_2^{\bullet-}$ ion is unstable and undergoes disproportionation reaction to form triiodide ion ($2I_2^{\bullet-} \rightarrow I_3^- + I^-$).[11] Thanks to this chemical step, the recombination of electrons in TiO_2 and $I_2^{\bullet-}$ does not occur to a large extent and contributes to a large conversion efficiency of DSSCs (11.1%).[12] The main disadvantage of the chemical modification approach is the loss of electron energy (voltage) that can be extracted from the device (~0.75 V loss in DSSC).

Much less explored approach toward chemical modification of radical ions involves a simple protonation/deprotonation of radical ions. It is known that the acidic/basic properties of radical ions change relative to their neutral analogs: once oxidized, the compound becomes more acidic, while the reduced compound usually becomes more basic. These changes in acid/base properties of radical ions can be used to neutralize the charges formed upon photoinduced electron transfer and achieve LLCS.

Received: June 17, 2011
Revised: September 13, 2011
Published: September 14, 2011

ACS Publications © 2011 American Chemical Society

dx.doi.org/10.1021/jp2056909 | *J. Phys. Chem. A* 2011, 115, 11606–11614

Scheme 1. Structures of Model Compounds Used in This Study; SMe-NI-H Undergoes Proton-Coupled Electron Transfer (PCET), while SMe-NI-Me Undergoes Electron Transfer (ET)

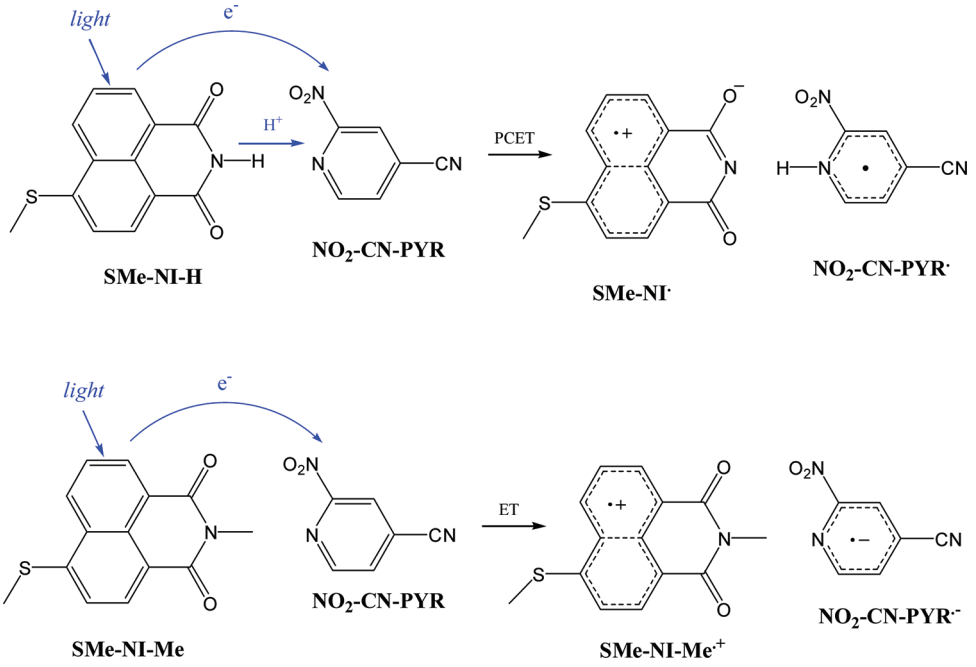

For example, Gust and Moore studied photoinduced charge separation in carotenoid/porphyrins/quinone (CPQ) triads to form long-lived $C^{\bullet+}PQ^{\bullet-}$ radical ions.[13] The authors found that the protonation of the reduced quinone radical anion to form $C^{\bullet+}PQH^{\bullet}$ drastically increases radical lifetimes (from 62 ns in nonprotonated to 2.5 μs in the protonated system). An example for LLCS using deprotonation of the oxidized donor has been reported by Hamachi and co-workers, who studied photoinduced electron transfer in a synthetic heme/$Ru(bpy)_3$/viologen triad incorporated in the myoglobin protein network.[14] The authors found that the lifetime of charge separated state increases 10^2-10^3 times if the oxidation of Fe-hydroxyl complex is accompanies by the deprotonation of the hydroxyl group (Fe^{III}—OH → Fe^{IV}=O).

In this study, we wish to expand on our understanding of proton-mediated electron transfer for achieving LLCS. As model compounds, we chose simple naphthalimide/pyridine donor/acceptor systems presented in Scheme 1. To ensure that the electron transfer flows from the naphthalimide to the pyridine, we incorporated electron-donating groups on naphthalimides (SMe-NI-H and SMe-NI-Me) and electron withdrawing groups on the pyridine (NO_2-CN-PYR). Based on pK_a values of pyridines and naphthalimides, photoinduced electron transfer from SMe-NI-H to NO_2-CN-PYR is expected to be accompanied by a proton transfer (PCET process in Scheme 1). Pyridines are known to significantly increase their basicity upon reduction. For example, pK_a value of 3-acetylpyridinium ion is 4.9, while the pK_a value of protonated 3-acetylpyridine radical is 13.4.[15] Imides have pK_a values in the 8−10 range,[16] and this value is expected to decrease upon one-electron oxidation. Based on these pK values, the proton transfer between neutral pyridines and naphthalimides cannot occur. However, the radical ions produced upon photoinduced electron transfer will undergo highly thermodynamically favored proton transfer: the pyridine radical anion is basic enough to remove a proton from oxidized naphthalimide radical cation. This PCET process is expected to produce neutral radicals that exhibit longer lifetimes than the corresponding charged radical ions. To investigate this possibility, we studied lifetimes of the radicals obtained in PCET process (SMe-NI-H) and compared them with lifetimes of the radical ions obtained during electron transfer process (ET in Scheme 1) using methylated SMe-NI-Me, which does not contain the acidic imide proton. In the previous study, we investigated the excited-state behavior of SMe-NI-H using femtosecond pump−probe spectroscopy in the UV/vis range.[17] In this study, we present the results of PCET and ET processes using naphthalimide/pyridine donor/acceptor systems. We report that the lifetimes of PCET radicals are longer than ET radical ions, thus demonstrating that PCET can be an excellent method for increasing the lifetimes of charge-separated species.

EXPERIMENTAL SECTION

Synthesis. 2-Cyano-4-nitro-pyridine was purchased from Sigma-Aldrich. All solvents were purchased from Fischer Scientific and used without further purification. Synthesis of SMe-NI-H was reported previously.[17] ^1H and ^{13}C NMR spectra were recorded using Bruker Avance 300 MHz spectrometer. GC-MS spectra were measured using Shimadzu GC-MS-Q5050A spectrometer.

***N*-Methyl-4-thiomethyl-naphthalimide (SMe-NI-Me).** SMe-NI-Me was prepared from 4-thiomethyl naphthalic anhydride in a reaction with methylamine. Syntheses of 4-thiomethyl naphthalic anhydride were described previously.[17] To a stirred solution of 4-thiomethyl naphthalic anhydride (0.2104 g, 0.8623 mmol) in 100 mL of methanol was added 5 mL of 37% solution of methylamine in ethanol. The mixture was heated for 3 h, cooled down and excess solvent was evaporated. The precipitate was collected and dried in the vacuum. Yield: 70%. MS-EI: m/z 257 [M^+ calcd

for $C_{14}H_{14}O_2NS$]. ^{1}H NMR (300 MHz, DMSO-d_6), δ ppm: 8.54 (dd, $J_{9,8}$ = 8.7 Hz, $J_{7,8}$ = 7.5 Hz, 2H), 8.39 (d, $J_{4,5}$ = 7.8 Hz, 1H), 7.91 (dd, $J_{8,7}$ = 7.5 Hz, $J_{8,9}$ = 8.7 Hz, 1H), 7.67 (d, $J_{5,4}$ = 7.8 Hz, 1H), 3.38 (s, 3H, -SCH_3), 2.74 (s, 3H, >N−CH_3); ^{13}C NMR (75 MHz, DMSO-d_6) δ ppm: 161.2, 161.0, 141.3, 131.4 (3-C), 130.9, 129.6, 126.6, 127.7, 127.6, 121.9, 118.6, 14.6 (-SCH_3), 12.1 (>N−CH_3).

Steady-State Spectroscopy. Absorption spectra were recorded on Agilent 8453 UV spectrometer in a 2 mm quartz cell. Fluorescence spectra were recorded on Edinburg Instruments Fluorimeter equipped with Xe900 lamp in 1 cm quartz cell. For fluorescence measurements, naphthalimide solutions were prepared with absorption of 0.05−0.1 at the excitation wavelength. SMe-NI-H and SMe-NI-Me were excited at 356 nm.

Binding Constant Determination. We evaluated the binding constant between SMe-NI-H and deuterated pyridine in $CDCl_3$ using ^{1}H NMR spectroscopy. A shift of the SMe-NI-H N-H peak was monitored as a function of varying concentrations of deuterated pyridine. Stock solutions of SMe-NI-H (c = 1.23 mM) and deuterated pyridine (c = 1.4 mM) in $CDCl_3$ were mixed in several different ratios and the shift of the N−H peak was plotted as a function of pyridine concentration. The binding constant was obtained using the following equation:[18]

$$\frac{1}{\Delta\delta} = \frac{1}{K\cdot\Delta\delta_{max}}\cdot\frac{1}{[\text{PYR-}d]} + \frac{1}{\Delta\delta_{max}}$$

where [PYR-d] is the concentration of deuterated pyridine, $\Delta\delta$ is a difference in the N−H chemical shift between SMe-NI-H in the presence and absence of PYR-d, $\Delta\delta_{max}$ is the difference in the N−H chemical shift between SMe-NI-H in chloroform and in pure PYR-d. The binding constant of K = 3 ± 1 M^{-1} was obtained for SMe-NI-H/pyridine complexation in chloroform.

Electrochemistry. Cyclic voltammograms were obtained at room temperature using a BAS Epsilon electrochemistry setup equipped with Pt-working electrode, nonaqueous Ag/Ag^+ reference electrode (0.01 M $AgNO_3$ in 0.1 M $N(C_4H_9)_4ClO_4$ chloroform solution), and Pt wire as an auxiliary electrode. Chloroform purification was achieved by passing it through a column filled with a mixture of $KMnO_4$ and alumina. The solvent was then distilled over CaH_2. For the electrochemical measurements, we used 2 mM solutions of naphthalimides and pyridines in 0.1 M $N(C_4H_9)_4ClO_4$ in chloroform. Prior to measurements, samples were degassed with argon. Cyclic voltammograms were measured using 100 mV/s sweep rate.

Spectroelectrochemistry was performed to obtain the absorption spectrum of NO_2−CN-PYR$^{\bullet-}$. The reduction of NO_2-CN-PYR (c = 2 mM in chloroform containing 0.1 M $N(C_4H_9)_4ClO_4$) was performed at the controlled potential of −1.22 V versus Fc (using Epsilon potentiostat). Electrodes used were as follows: working, gold mesh electrode; counter, Pt wire; reference, nonaqueous Ag^+/Ag electrode. The changes in the absorption spectra were recorded using Agilent 8453 UV spectrometer.

Pump−Probe Measurements. The laser system for the ultrafast transient absorption measurements was described elsewhere.[19] The 800 nm pulse was generated by a mode-locked Ti:Sapphire laser (Hurricane, Spectra-Physics) at 1 kHz frequency. The pulse width (∼110 fs) was determined by autocorrelator (Positive Light). The beam output from Hurracane was split into pump (85%) and probe (8%) beams. The pump beam was sent through second harmonics generator (Super Tripler, CSK) to obtain a 400 nm excitation source (pump). The energy of the pump was 2 μJ/pulse. The probe beam was sent through the delay stage (MM 4000, Newport) and then focused into a CaF_2 crystal for white light continuum generation between 350 and 770 nm. The sample concentrations were 0.4−0.5 mM in chloroform (HPLC grade, stabilized by amylene). The flow cell (Spectrocell Inc., 0.7 mL volume with 2 mm path length), pumped by a Fluid Metering RHSY Lab pump (Scientific Support Inc.), was used to prevent photodegradation. Transient absorption spectra were collected using a CCD camera (Ocean Optics, S2000).

Data Processing and Analysis. (i) Chirp correction was determined using nonresonant optical Kerr effect (OKE) measurements;[20] (ii) Noise was reduced using a singular value decomposition (SVD) method using a code written in Matlab 7.1; (iii) Transient absorption data were analyzed using SPECFIT/32 Global Analysis System (Spectrum Software Associates, MA, U.S.A.). This program allows a decomposition of transient absorption data using kinetic models. The analysis is achieved by a global analysis method that uses singular value decomposition method to reduce the size of the fitted data.[21] First, we performed global analysis of the data to determine the sufficient number of decay components and obtain the decay-associated difference spectra (DADS). Once we obtained the decay lifetimes, we applied a series of models and the goodness of the fit was judged using the value of root-mean-square error. This procedure provided species-associated difference spectra (SADS) presented in this manuscript.

DFT Calculations. All computations were performed at the Ohio Supercomputer Center. Geometry optimizations were performed using Gaussian 03[22] with Becke's three-parameter hybrid exchange functional with Lee−Yang−Parr correlation functional (B3LYP).[23] We used 6-31+G* basis set[24] and the solvent effect (chloroform) was calculated using polarizable continuum model (PCM).[25−28] All stationary points were confirmed to be energy minima using vibrational frequency calculations (B3LYP/6-31+G*), which showed that all of the computed vibrational frequencies were nonimaginary. Vertical transition energies and difference density plots were then calculated at the TD-B3LYP/6-31+G* level of theory.[29]

RESULTS AND DISCUSSION

Excited-State Behavior of Nahpthalimides. In the previous study, we investigated the excited state behavior of a series of naphthalimide derivatives, including SMe-NI-H.[17] We found that the photophysics of SMe-NI-H are dictated by two close-lying excited states: (i) $^1n,\pi^*$ (S_2) state in which the nonbonding oxygen electrons of the imide moiety are promoted to the π^* orbital of the naphthalimide, and (ii) $^1\pi,\pi^*$ (S_1) state with a significant charge transfer character (-SMe group acts as an electron donor). Pump−probe experiments showed that the initially produced S_2 ($^1n,\pi^*$) state quickly decays to for form a long-lived S_1 ($^1\pi,\pi^*$) state with charge transfer character.

For our current studies of photoinduced electron transfer between naphthalimides and NO_2-CN-PYR, it is important to show that methylated and protonated naphthalimides exhibit the same excited-state behavior. This assures that the only difference in the electron transfer dynamics of methylated and protonated naphthalimides is caused by the proton motion in the case of protonated systems. Thus, we present here a careful comparison of the photophysics of the methylated naphthalimide SMe-NI-Me with the previously studied protonated analog SMe-NI-H. Figure 1 presents absorption and fluorescence spectra of the two

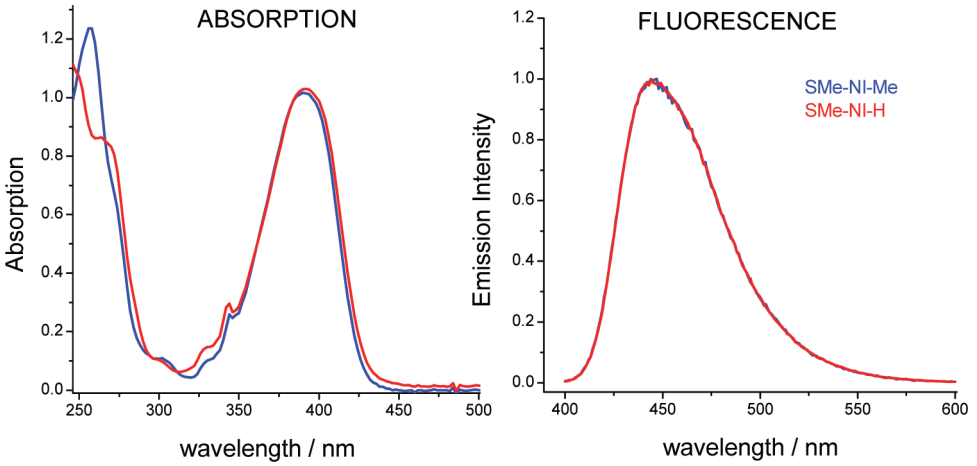

Figure 1. Normalized absorption and fluorescence spectra of SMe-NI-Me and SMe-NI-H in CH_2Cl_2 (c = 60 μM). Excitation wavelengths for fluorescence spectra was λ = 390 nm for SMe-NI-H and SMe-NI-Me.

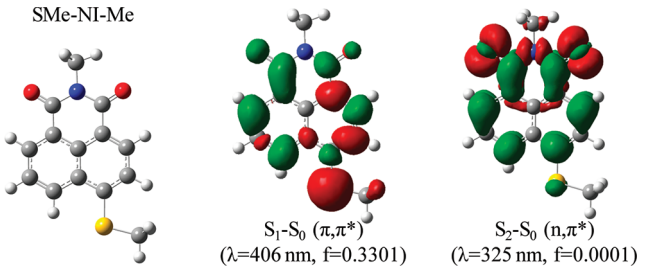

Figure 2. S_1-S_0 and S_2-S_0 difference density plots for SMe-NI-Me obtained using B3LYP/6-31+G* (PCM model for chloroform) methodology. Atom labels: carbon (gray); oxygen (red); nitrogen (blue); sulfur (yellow); hydrogen (white). Red color represents the depletion of the electron density in the excited state, while green represents accumulation of the electronic density in the excited state.

naphthalimides. The absorption (fluorescence) of −SMe derivatives appear at 390 nm (445 nm), and the methylated and protonated derivatives exhibit almost identical spectral features.

To assign the excited-state character of the methylated derivative, we performed time-dependent density functional theory (TD DFT)[29] calculations for SMe-NI-Me using B3LYP/6-31+G* (PCM model for chloroform) methodology.[23,24,30,31] The calculated lowest-energy electronic transition (406 nm for SMe-NI-Me) correlates well with the experimental absorption band (390 nm for SMe-NI-Me) for naphthalimide derivatives. The calculated transition energy is lower than the experimental absorption band by ∼0.1 eV, which is within the typical 0.1−0.5 eV error expected for TD DFT calculations.[32] The character of the lowest excited states of SMe-NI-Me can be evaluated using S_n-S_0 difference-density plots (DDPs) presented in Figure 2. The lowest S_1 state can be characterized as a charge transfer π,π^* state, in which the electronic charge is transferred from the −SMe group (red color in DDPs represents the depletion of charge in the excited state) to the naphthalimide moiety (green color represents the accumulation of charge). The S_2 state exhibits low oscillator strength (Figure 2), which is characteristic of the n,π^* state. In addition, DDP for S_2 state of methylated naphthalimide confirms the n,π^* assignment: a depletion of electronic charge from the oxygen atoms of the imide moiety and the accumulation of the charge density on the π system of the naphthalimide. This assignment of SMe-NI-Me excited states is identical to our previous assignment of excited states in SMe-NI-H,[17] which provides additional evidence that methylation of naphthalimides does not alter their excited state behavior.

We further compared the excited-state dynamics of methylated and protonated naphthalimides using visible pump−probe spectroscopy. Figure 3a shows the changes that occur in the first 10 ps after the 400 nm excitation of SMe-NI-Me. At t = 0 ps, the transient spectrum is dominated by the absorption band at 470 nm. Within 10 ps, the absorption maximum shifts to lower wavelength (450 nm), and a stimulated emission signal appears at 510 nm. At delays longer than 10 ps, we observed no spectral changes and only a slight decrease of the overall signal occurred by 1300 ps (data not shown). These spectral features are identical with the transient absorption spectra obtained previously for SMe-NI-H.[17] In analogy to the SMe-NI-H results, we assign the t = 0 ps component to the S_2 state of SMe-NI-Me (with $^1n,\pi^*$ character) and the 10 ps component to the S_1 state of SMe-NI-Me (with $^1\pi,\pi^*$ charge-transfer character). Using global target analysis (see Experimental Section for more details), we obtained the spectral features of two states (Figure 3b). The lifetime of S_2 state is short (4 ps), and we assign this decay to $S_2 \rightarrow S_1$ internal conversion. The S_1 state decays with two lifetime components (30 ps and ∼6 ns). The long 6 ns component is assigned to $S_1 \rightarrow S_0$ radiative decay, while the origin of the 30 ps component is not clear (it might be caused by the presence of more than one SMe-NI-Me conformer in the solution).

To compare the excited state behavior of SMe-NI-H and SMe-NI-Me, Figure 3c presents the decays at 500 nm recorded for the two compounds. Both decays are almost identical, consisting of the positive signal at t = 0 due to the absorption of the S_2 state, which decays with a 4 ps lifetime to a negative signal due to stimulated emission of the S_1 state. Both decay traces fit well using three lifetimes (4 ps, 40 ps, and 6 ns). The only difference between the two decay traces is in the amplitude of the decay components. Thus, these results further demonstrate that SMe-NI-H and SMe-NI-Me exhibit almost identical excited-state behavior.

Electrochemistry. The driving force for photoinduced electron transfer between naphthalimides and NO_2-CN-PYR was evaluated using oxidation and reduction potentials obtained using cyclic voltammetry. As can be seen from Figure 4A, cyclic

dx.doi.org/10.1021/jp2056909 |J. Phys. Chem. A 2011, 115, 11606–11614

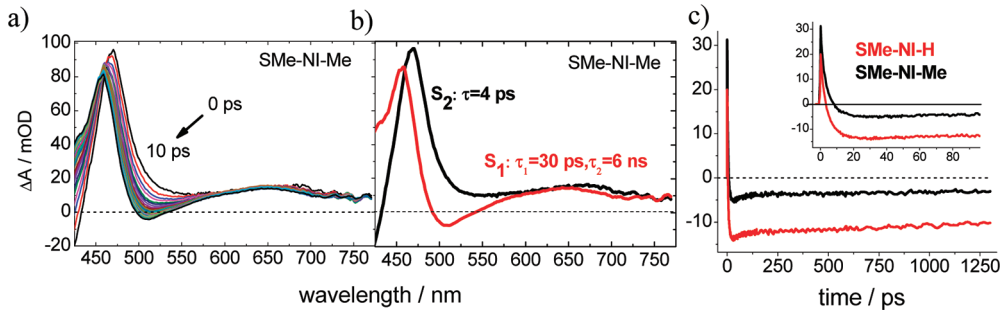

Figure 3. (a) Transient absorption spectra of SMe-NI-Me in chloroform (c = 0.4 mM) obtained at 0−10 ps delays after the 400 nm excitation pulse; (b) spectra and lifetimes of two SMe-NI-Me components obtained using global analysis; (c) decays at 500 nm obtained for SMe-NI-H (red) and SMe-NI-Me (black).

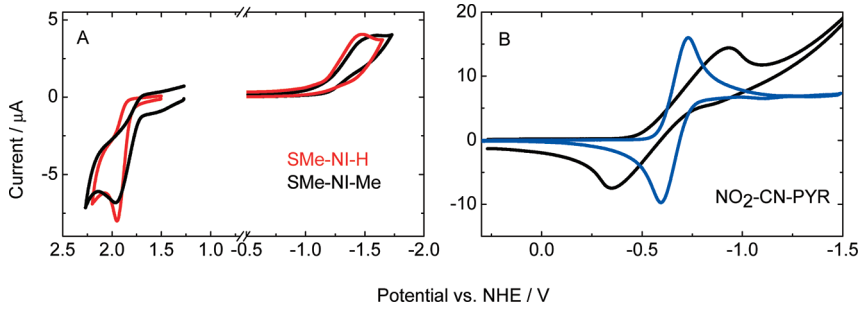

Figure 4. (A) Cyclic voltammograms of SMe-NI-H (red) and SMe-NI-Me (black) in chloroform (c = 1 mM). (B) Cyclic voltammograms for NO_2-CN-PYR (c = 2 mM) in chloroform (black) and acetonitrile (blue). Tetrabutyl-ammonium perchlorate was used as a supporting electrolyte. Sweep rate: 100 mV/s. Working electrode: platinum; counter electrode: platinum wire; reference electrode: Ag/Ag^+ (nonaqueous).

voltammograms of both SMe-NI-H and SMe-NI-Me exhibit a reduction peak at E_c = −1.46 V and an oxidation peak at E_a = +1.95 V versus NHE. All of these peaks are chemically irreversible at the sweep rate of 100 mV/s. Previous studies of unsubstituted naphthalimides showed that they exhibit a one-electron reduction to form the naphthalimide radical anion[33] in the −1.00 to −1.10 V range, which displays a varying degree of chemical reversibility in different systems.[34,35] On the other hand, the oxidation of unsubstituted naphthalimides has not been studied before, because it occurs at a high potential (E^0 > 2 V). For this reason, naphthalimides are generally used as electron acceptors,[36] not donors. Because we are interested in using naphthalimides as electron donors, we added electron-donating groups to the naphthalimide moiety to decrease the oxidation potential. As expected, electron-donating −SMe substituent decreases the oxidation potential of naphthalimides to +1.95 V.

The reduction of NO_2-CN-PYR occurs at −0.64 V, showing a chemically reversible and electrochemically irreversible wave (Figure 4B). We performed measurements using acetonitrile as a solvent (Figure 4b, blue curve) and found a reduced degree of electrochemical reversibility for the NO_2-CN-PYR reduction peak at −0.64 V. Due to the presence of electron-withdrawing substituents, the reduction potential of NO_2-CN-PYR occurs at a significantly less negative potential than the reduction of the unsubstituted pyridine (E^0 = −2.76 V in DMF[37]). Using these electrochemical and spectroscopic data, we estimated the thermodynamic driving force for photoinduced electron transfer between naphthalimides and NO_2-CN-PYR (Table 1). The estimated ΔG values demonstrate that the photoinduced electron transfer between excited SMe-NI-H (SMe-NI-Me) is favored by −0.39 eV, while the ΔG for charge recombination is −2.59 eV.

Table 1. Estimates of the Driving Force for Photoinduced Electron Transfer and Geminate Recombination between Naphthalimides and NO_2-CN-PYR

	E_{ox}[a] (V)	E_{oo}[b] (eV)	ΔG_f[c] (eV)	ΔG_b[d] (eV)
SMe-NI-H	1.95	2.98	−0.39	−2.59
SMe-NI-Me	1.95	2.98	−0.39	−2.59

[a] Because the oxidation potential is chemically irreversible, we tabulated the potentials of anodic peaks from cyclic voltammograms. [b] S_1-S_0 energy gap (E_{00}) was calculated as a half point between absorption and fluorescence maxima (Figure 1). [c] Calculated using Rehm−Weller equation:[43] $\Delta G_f = (E_{ox} - E_{red}) - E_{oo}$, where E_{red} = −0.64 V (reduction potential of NO_2-CN-PYR. [d] Calculated using $\Delta G_b = E_{red} - E_{ox}$.

Spectroelectrochemistry was performed to determine the spectral features of radicals involved in the electron transfer. Figure 5 shows the spectrum of NO_2−CN-PYR radical anion obtained upon reduction of NO_2-CN-PYR at −1.0 V versus NHE. Before electrolysis, the absorption spectrum of NO_2-CN-PYR consists of a band with a maximum at 280 nm. During electrolysis, we observe the growth of new absorption bands with maxima at 270, 325, and 480 nm, which we assign to the absorption of NO_2-CN-PYR radical anion (NO_2-CN-PYR$^{\bullet-}$). Thus, in our studies of photoinduced electron transfer using transient absorption, we expect to observe the growth of an absorption band at 480 nm. In our studies of PCET, we expect the formation of neutral NO_2-CN-PYR radical (NO_2-CN-PYR-H$^{\bullet}$), whose spectrum is not known. However, we expect that the spectrum of neutral radical is similar to the spectrum of radical anion presented in Figure 7. For example, the absorption spectrum of

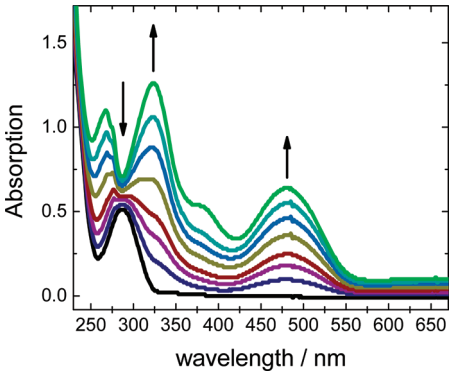

Figure 5. Absorption spectra of NO_2-CN-PYR (c = 2 mM) in chloroform obtained at different time delays during electrolysis at −1.0 V vs NHE. Working electrode: Pt mesh; counter electrode: Pt wire; reference electrode: Ag/Ag^+. Time delays: from black to light green: 0, 1, 2, 3, 5, 7, 9, and 20 min.

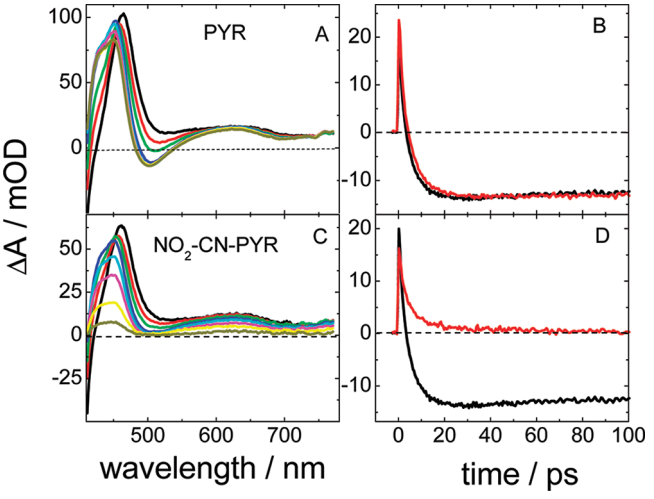

Figure 6. Transient absorption spectra of SMe-NI-H (c = 0.4 mM) in the presence of 0.5 M pyridine (A) and 0.5 M NO_2-CN-PYR (C) in chloroform. Spectra were obtained at several time delays following the 400 nm excitation pulse: 0 (black), 2.5 (red), 4 (green), 12 (blue), 29 (light blue), 63 (magenda), 160 (yellow), and 360 ps (dark green). (B and D) Decays of SMe-NI-H signal at 500 nm. The black curve in both panels represents the decay of SMe-NI-H signal in the absence of pyridine. The red curve in (B) represents decay of SMe-NI-H in the presence of pyridine, while the red curve in (D) represents the decay of SMe-NI-H in the presence of NO_2-CN-PYR.

4-carbamylpyridinyl radical anion (~390 nm) is slightly blue-shifted relative to the absorption spectrum of its conjugate acid (410 nm).[38] We also attempted to obtain the spectrum of radical cations of naphthalimides by performing spectroelectrochemical measurements during anodic oxidation of SMe-NI-H. However, we were unable to record the absorption spectra due to chemical instability of these radical cations. Based on the previous studies with naphthalene radical cation, we expect the radical cations of naphthalimides to exhibit very week absorption in the visible range.[39] Thus, we do not anticipate to observe these transients in our transient absorption measurements.

Photoinduced Electron Transfer. Photoinduced electron transfer between SMe-NI-H and NO_2-CN-PYR was studied using pump−probe spectroscopy (Figure 6C,D). In the presence of NO_2-CN-PYR, transient absorption signal of SMe-NI-H decays faster at all probe wavelengths, which is consistent with the electron transfer process from excited SMe-NI-H to NO_2-CN-PYR. The most drastic change is observed at 500 nm, where SMe-NI-H in the absence of NO_2-CN-PYR exhibits stimulated emission (Figure 6D, black curve). In the presence of NO_2-CN-PYR, the stimulated emission signal does not appear, and instead a positive signal persists for ~20 ps (Figure 6D, red curve). Based on spectroelectrochemical measurements (Figure 5), we assign the transient signal at 500 nm to the NO_2-CN-PYR radical. To confirm that the photoinduced electron transfer to NO_2-CN-PYR is responsible for changes in the SMe-NI-H signal, we performed pump−probe experiments on SMe-NI-H in the presence of pyridine. Pyridine is similar in structure to NO_2-CN-PYR, but its reduction potential is too negative for photoinduced electron transfer from excited SMe-NI-H to take place (the reduction potential of pyridine is −2.76 V,[37] the driving force for the electron transfer between excited SMe-NI-H/SMe-NI-Me and pyridine is ΔG = + 1.73 eV). As expected, the excited-state behavior of SMe-NI-H does not change if pyridine is added to the solution (Figure 6A,B). These results confirm that the deactivation of SMe-NI-H excited state in the presence of NO_2-CN-PYR is caused by photoinduced electron transfer and not some other deactivation pathway, such as excited-state deprotonation of the N−H proton in SMe-NI-H.

We investigated the electron transfer dynamics at several NO_2-CN-PYR concentrations (Figure 7). The rate of electron transfer is concentration-dependent, suggesting that the process is diffusion-controlled. This result suggests that the hydrogen-bonded complex between SMe-NI-H and NO_2-CN-PYR does not form at the appreciable degree, and is consistent with the low association constant for the formation of SMe-NI-H/pyridine complex (K = 3 M^{-1}) determined using ^{1}H NMR spectroscopy (see Experimental Section for more information). We were not able to determine the association constant for SMe-NI-H/NO_2-CN-PYR complex due to the overlap of the N−H proton signal of SMe−NI-H with the proton signals of NO_2-CN-PYR. However, due to the electron-withdrawing nature of nitro and cyano substituents of NO_2-CN-PYR, we predict that this binding constant is even lower than the K = 3 M^{-1} we obtained in the case of pyridine. Thus, the electron transfer process studied here does not involve the electron transfer of the preassociated complex.

The occurrence of PCET in SMe-NI-H/NO_2-CN-PYR was investigated by comparing the dynamics of SMe-NI-H decay with those of SMe-NI-Me. In contrast to SMe-NI-H, which can undergo PCET, the methylated SMe-NI-Me does not have acidic protons and can perform only an electron transfer process. Figure 8 compares the decays of SMe-NI-H and SMe-NI-Me transient absorption signals in the presence of high concentration of NO_2-CN-PYR. At 625 nm, the only absorbing species is the excited SMe-NI-H (or SMe-NI-Me). Thus, the decay at this wavelength is associated with the rate of the forward electron transfer. As can be seen from Figure 8A, the decays of SMe-NI-H and SMe-NI-Me are similar, with a slightly faster decay in the case of SMe-NI-Me. Both decays were fit to a biexponential function: lifetimes for SMe-NI-H were τ_1 = 40 ps and τ_2 = 903 ps, while those for SMe-NI-Me were τ_1 = 40 ps and τ_2 = 667 ps. The 40 ps component is present in all SMe-NI-H samples and was discussed previously. The lifetimes τ_2 are associated with the diffusion-controlled photoinduced electron transfer between SMe-NI-H (or SMe-NI-Me) and NO_2-CN-PYR, and show that the rate is similar, but slightly faster in the case of SMe-NI-Me.

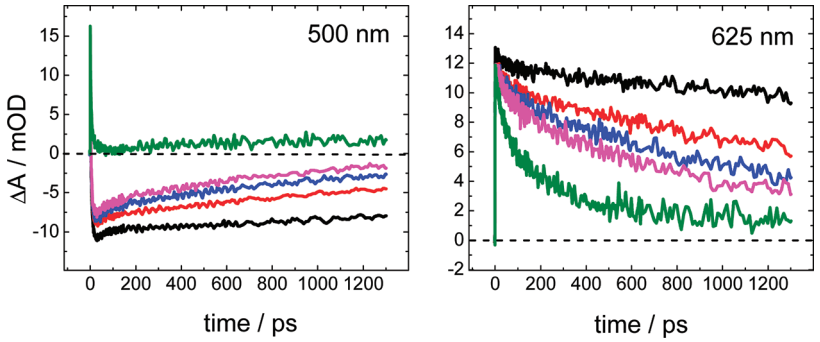

Figure 7. Excited-state decays of SMe-NI-H (c = 0.5 mM in chloroform) in the presence of varying concentrations of NO_2-CN-PYR: 0 (black), 0.0625 (red), 0.125 (blue), 0.25 (magenda), and 0.5 M (olive). Samples were excited using 400 nm pump beam.

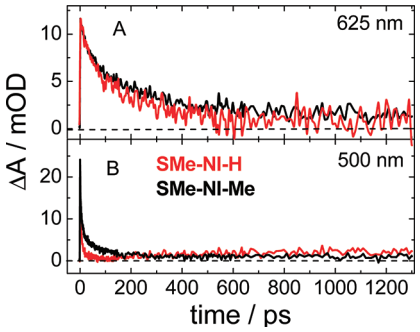

Figure 8. Decay of transient absorption signal of 0.4 mM SMe-NI-H (red) and SMe-NI-Me (black) in the presence of 0.5 M NO_2-CN-PYR. Samples were excited using 400 nm pump beam and the decays were monitored at 625 (A) and 500 nm (B).

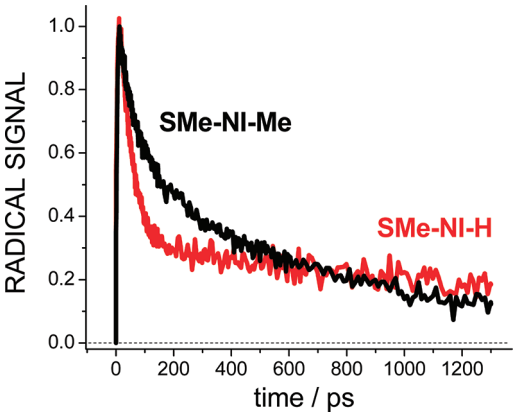

Figure 9. Dynamics of the NO_2-CN-PYR radical (or radial anion) signal obtained in the presence of SMe-NI-H (red) and SMe-NI-Me (black). The signal was obtained using the following equation: $S^R = S_{wp}^{500} - (S_{np}^{500})/(S_{np}^{625})S_{wp}^{625}$, where S_{wp} represents decay of SMe-NI-H (or SMe-NI-Me) signal in the presence of NO_2-CN-PYR and S_{np} represents the decay in the absence of NO_2-CN-PYR. The decays were obtained at 500 and 625 nm.

Table 2. Rates of Forward and Back Electron Transfer between SMe-NI-H or SMe-NI-Me and NO_2-CN-PYR (c = 0.5 M)

	k_f (s^{-1})	k_{b1} (s^{-1})	k_{b2} (s^{-1})
SMe-NI-H	1.1×10^9	2.3×10^{10}	4.3×10^8
SMe-NI-Me	1.5×10^9	1.3×10^{10}	1.2×10^9

Given the similarity in the decay dynamics ($k_f = 1.1 \times 10^9$ s^{-1} for SMe-NI-H and $k_f = 1.5 \times 10^9$ s^{-1} for SMe-NI-Me, Table 2), we conclude that both processes involve only a transfer of the electron, without the accompanying proton transfer. The small difference in the electron transfer rates between SMe-NI-H and SMe-NI-Me can be assigned to a larger electronic coupling constant for electron transfer between SMe-NI-Me and NO_2-CN-PYR.

The charge recombination rates were obtained from the decays of SMe-NI-H/SMe-NI-Me signals at 500 nm (Figure 8B). The transient absorption at this wavelength arises due to three signals: (i) excited-state absorption due to S_2 state of SMe-NI-H (or SMe-NI-Me); (ii) stimulated emission due to S_1 state of SMe-NI-H (or SMe-NI-Me); (iii) the absorption due to NO_2-CN-PYR radical (or radical anion). The absorption by radical cation of SMe-NI-H (or SMe-NI-Me) is not expected to be detectable via transient absorption, as illustrated in previous studies of radical cations of similar naphthalimide derivatives.[40] We extracted the contribution due to NO_2-CN-PYR radical by subtracting the contribution from S_1 and S_2 states of SMe-NI-H/SMe-NI-Me. For this purpose, we assumed that the decay at 625 nm arises purely due to SMe-NI-H excited state. We scaled and subtracted this contribution from the decay at 500 nm, and the NO_2-CN-PYR radical signal obtained using this approach is presented in Figure 9. We used this approach in previous studies of photoinduced electron transfer in micelles and liquids to extract the dynamics of the Rhodamine B radical.[41,42] As can be seen from Figure 9, the decays of NO_2-CN-PYR$^{\bullet-}$ (formed in the presence of SMe-NI-Me) and neutral NO_2-CN-PYRH$^{\bullet}$ (formed in the presence of SMe-NI-H) are different. Both signals decay biexponentially with lifetimes of τ_1 = 44 ps and τ_2 = 2340 ps in the case of SMe-NI-H and of τ_1 = 75 ps and τ_2 = 835 ps in the case of SMe-NI-Me. We assign the shorter τ_1 component to recombination of radical pairs at a contact distance (in the solvent cage), while the longer-lived component τ_2 possibly arises due to the diffusion-limited recombination of the solvent-separated radicals. The values for charge recombination in the solvent cage for SMe-NI-H and SMe-NI-Me are similar (k_{b1} values in Table 2). Thus, we assign this process to the electron recombination between radical ions, without the accompanying proton transfer. On the other hand, the recombination of solvent-separated radical pairs exhibits and opposite trend: τ_2 component is longer-lived in the case of SMe-NI-H, which we assign to be due to proton-coupled electron transfer.

Scheme 2 outlines electron transfer and proton-coupled electron transfer processes that occur in our study. We postulate

dx.doi.org/10.1021/jp2056909 |J. Phys. Chem. A 2011, 115, 11606–11614

Scheme 2. Proposed Electron Transfer and Proton-Coupled Electron Transfer Processes between SMe-NI-H/SMe-NI-Me and NO_2-CN-PYR

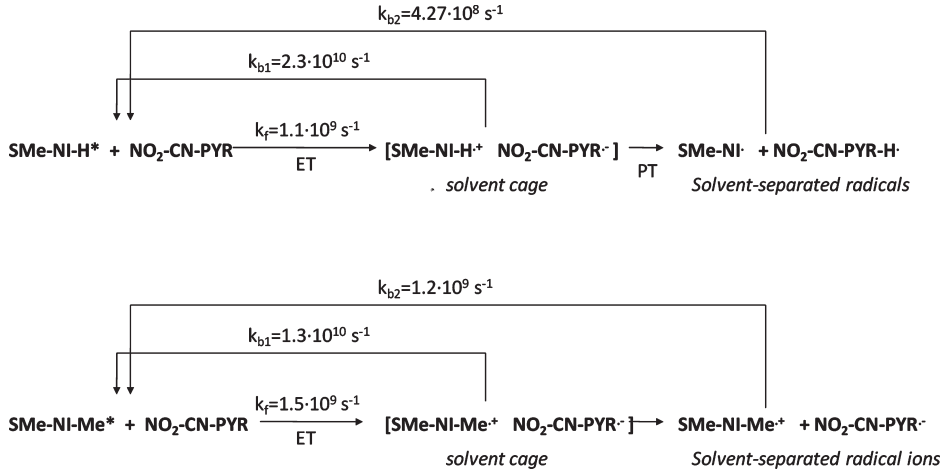

that the photoinduced electron transfer between excited SMe−NI-H (or SMe-NI-Me) and NO_2−CN-PYR forms solvent-caged radical ion pairs with a rate of $k_f \sim 1 \times 10^{10}$ s^{-1}. Even though SMe-NI-H offers the possibility of the proton-coupled process, we conclude that the proton transfer does not occur during this early charge-transfer process. This conclusion is based on the similarity between k_f values in SMe-NI-H and SMe-NI-Me model compounds. The possible reason for the lack of proton transfer during the initial electron transfer process is the unfavorable orientation of the imide N−H group relative to the pyridine N-atom. For efficient electron transfer, the donor/acceptor aromatic moieties are oriented in the π-stacked geometry. At this geometry, the proton transfer will not be favored, due to large distance and unfavorable orientation between N−H moiety of SMe-NI-H and aromatic N-atom of NO_2-CN-PYR. Once the solvent-caged radical ions are formed, some of them recombine with the rate of $k_{b1} \sim 1-2 \times 10^{10}$ s^{-1}. Some radical ions escape the solvent cage and their recombination occurs at a lower rate k_{b2}. In this case, we observe an interesting reversal of rates constant values: the recombination rate becomes slower in the case of SMe-NI-H, suggesting that the solvent-separated ion-pairs undergo proton transfer process to produce neutral radicals. Because the neutral radicals formed upon proton transfer are not attracted to each other by electrostatic interactions, their recombination is slower than the recombination of the charged radical ions produced from SMe-NI-Me. This results in a significant reduction of the k_{b2} values in the case of SMe-NI-H ($k_{b2} = 4.3 \times 10^8$ s^{-1}) relative to that of SMe-NI-Me ($k_{b2} = 1.2 \times 10^9$ s^{-1}).

CONCLUSIONS

We compared the recombination rates of radicals produced in two model systems: (i) SMe-NI-Me and NO_2-CN-PYR, where photoinduced electron transfer produces charged radical ions, and (ii) SMe-NI-H and NO_2-CN-PYR, where proton-coupled electron transfer produces neutral radicals. We initially compared the electronic properties of SMe-NI-H and SMe-NI-Me to demonstrate that the two derivatives exhibit very similar electrochemical and excited-state behavior. Based on their similar electronic properties, we conclude that SMe-NI-H and SMe-NI-Me can be used to study the effect of proton transfer on the rates of radical recombination. Using ultrafast pump−probe spectroscopy, we obtained the rates of forward and back electron transfer in the two model systems. We found that the initial charge separation involves electron transfer to produce radical ion pairs in the solvent cage (with a rate of $\sim 1 \times 10^9$ s^{-1}). A portion of solvent-caged radical ions quickly recombine (with a rate of $\sim 1 \times 10^{10}$ s^{-1}). We postulate that the proton transfer does not occur during these early time events, possibly due to unfavorable orientation of SMe-NI-H and NO_2-CN-PYR. However, a portion of radical ions manage to escape the solvent cage and they recombine at the longer time scale. This process appears to be accompanied by the proton transfer in the case of SMe-NI-H, producing neutral radical pairs. We find that the recombination rate is slower in the case of SMe-NI-H (4.27×10^8 s^{-1}) than in the case of SMe-NI-Me (1.2×10^9 s^{-1}), and we attribute this difference to the lack of electrostatic attraction between the neutral radicals in the case of SMe-NI-H. Our results demonstrate that the proton-coupled electron transfer can be successfully used to achieve long-lived charge separation in the light-driven donor−acceptor systems.

AUTHOR INFORMATION

Corresponding Author

*E-mail: kglusac@bgsu.edu.

ACKNOWLEDGMENT

This research is supported by ACS PRF (Grant No. 46807-G4). We thank Ohio Supercomputer Center for computational resources and Prof. Felix Castellano for his help with spectroelectrochemical measurements.

REFERENCES

(1) Blankenship, R. E. *Molecular Mechanisms of Photosynthesis*; Blackwell Science: New Jersey, 2002.
(2) Wasielewski, M. R. *Chem. Rev.* **1992**, *92*, 435–461.
(3) Gust, D.; Moore, T. A.; Moore, A. L. *Acc. Chem. Res.* **2001**, *34*, 40–48.
(4) Meyer, T. J. *Acc. Chem. Res.* **1989**, *22*, 163–170.
(5) Marcus, R. A. *Annu. Rev. Phys. Chem.* **1964**, *15*, 155–196.

(6) Imahori, H.; Tamaki, K.; Guldi, D. M.; Luo, C. P.; Fujitsuka, M.; Ito, O.; Sakata, Y.; Fukuzumi, S. *J. Am. Chem. Soc.* **2001**, *123*, 2607–2617.
(7) Fukuzumi, S.; Nakanishi, I.; Suenobu, T.; Kadish, K. M. *J. Am. Chem. Soc.* **1999**, *121*, 3468–3474.
(8) Ma, W. L.; Yang, C. Y.; Gong, X.; Lee, K.; Heeger, A. J. *Adv. Funct. Mater.* **2005**, *15*, 1617–1622.
(9) Chen, H. Y.; Hou, J. H.; Zhang, S. Q.; Liang, Y. Y.; Yang, G. W.; Yang, Y.; Yu, L. P.; Wu, Y.; Li, G. *Nat. Photon.* **2009**, *3*, 649–653.
(10) Oregan, B.; Gratzel, M. *Nature* **1991**, *353*, 737–740.
(11) Boschloo, G.; Hagfeldt, A. *Acc. Chem. Res.* **2009**, *42*, 1819–1826.
(12) Chiba, Y.; Islam, A.; Watanabe, Y.; Komiya, R.; Koide, N.; Han, L. Y. *Jpn. J. Appl. Phys., Part 2* **2006**, *45*, L638–L640.
(13) Hung, S. C.; Macpherson, A. N.; Lin, S.; Liddell, P. A.; Seely, G. R.; Moore, A. L.; Moore, T. A.; Gust, D. *J. Am. Chem. Soc.* **1995**, *117*, 1657–1658.
(14) Hu, Y. Z.; Tsukiji, S.; Shinkai, S.; Oishi, S.; Hamachi, I. *J. Am. Chem. Soc.* **2000**, *122*, 241–253.
(15) Bruhlman, U; Hayon, E. *J. Am. Chem. Soc.* **1974**, *96*, 6169–6175.
(16) Hargreav, Mk; Pritchar, Jg; Dave, H. R. *Chem. Rev.* **1970**, *70*, 439.
(17) Kucheryavy, P.; Li, G. F.; Vyas, S.; Hadad, C.; Glusac, K. D. *J. Phys. Chem. A* **2009**, *113*, 6453–6461.
(18) Wong, K. F.; Ng, S. *Spectrochim. Acta, Part A* **1976**, *32*, 455–456.
(19) Li, G.; Glusac, K. D. *J. Phys. Chem. A* **2008**, *112*, 4573–4583.
(20) Yamaguchi, S.; Hamaguchi, H. O. *Appl. Spectrosc.* **1995**, *49*, 1513–1515.
(21) Gampp, H.; Maeder, M.; Meyer, C. J.; Zuberbuhler, A. D. *Talanta* **1985**, *32*, 95–101.
(22) Frisch, M. J.; Trucks, G. W.; Schlegel, H. B.; Scuseria, G. E.; Robb, M. A.; Cheeseman, J. R.; Montgomery, J. A., Jr.; Vreven, T.; Kudin, K. N.; Burant, J. C., et al. *Gaussian 03*, Revision C.02; Gaussian, Inc.: Wallingford CT, 2004.
(23) Becke, A. D. *J. Chem. Phys.* **1993**, *98*, 5648–5652.
(24) Francl, M. M.; Pietro, W. J.; Hehre, W. J.; Binkley, J. S.; Gordon, M. S.; Defrees, D. J.; Pople, J. A. *J. Chem. Phys.* **1982**, *77*, 3654–3665.
(25) Tomasi, J.; Persico, M. *Chem. Rev.* **1994**, *94*, 2027–2094.
(26) Cossi, M.; Barone, V. *J. Chem. Phys.* **1998**, *109*, 6246–6254.
(27) Barone, V.; Cossi, M.; Tomasi, J. *J. Comput. Chem.* **1998**, *19*, 404–417.
(28) Cramer, C. J.; Truhlar, D. G. *Chem. Rev.* **1999**, *99*, 2161–2200.
(29) Olivucci, M. *Computational Photochemistry*; Elsevier: Amsterdam, 2005; pp 92−128.
(30) Becke, A. D. *Phys. Rev. A* **1988**, *38*, 3098–3100.
(31) Lee, C. T.; Yang, W. T.; Parr, R. G. *Phys. Rev. B* **1988**, *37*, 785–789.
(32) Dreuw, A.; Head-Gordon, M. *Chem. Rev.* **2005**, *105*, 4009–4037.
(33) Nelsen, S. F. *J. Am. Chem. Soc.* **1967**, *89*, 5925.
(34) McAdam, C. J.; Robinson, B. H.; Simpson, J.; Tagg, T. *Organometallics* **2010**, *29*, 2474–2483.
(35) McAdam, C. J.; Morgan, J. L.; Robinson, B. H.; Simpson, J.; Rieger, P. H.; Rieger, A. L. *Organometallics* **2003**, *22*, 5126–5136.
(36) Altieri, A.; Gatti, F. G.; Kay, E. R.; Leigh, D. A.; Martel, D.; Paolucci, F.; Slawin, A. M. Z.; Wong, J. K. Y. *J. Am. Chem. Soc.* **2003**, *125*, 8644–8654.
(37) Baumgartel, H.; Retzlav, K.-J. *Encyclopedia of Electrochemistry of the Elements*; M. Dekker: New York, 1973; Vol. XV, p 194.
(38) Tripathi, G. N. R.; Su, Y. L.; Bentley, J.; Fessenden, R. W.; Jiang, P. Y. *J. Am. Chem. Soc.* **1996**, *118*, 2245–2256.
(39) Gschwind, R.; Haselbach, E. *Helv. Chim. Acta* **1979**, *62*, 941–955.
(40) Aveline, B. M.; Matsugo, S.; Redmond, R. W. *J. Am. Chem. Soc.* **1997**, *119*, 11785–11795.
(41) Glusac, K.; Goun, A.; Fayer, M. D. *J. Chem. Phys.* **2006**, *125*.
(42) Goun, A.; Glusac, K.; Fayer, M. D. *J. Chem. Phys.* **2006**, *124*.
(43) Rehm, D.; Weller, A. *Isr. J. Chem.* **1970**, *8*, 259–71.